Biophysical Reviews and Letters, Vol.1, No.4 (2006) 375-386

Biophysical Reviews and Letters

INFLUENCE OF TRANSPORT RATES ON THE PROTEIN DEGRADATION BY PROTEASOMES

A. ZAIKIN, A.K. MITRA, D.S. GOLDOBIN, J. KURTHS

Institute of Physics, Potsdam University, Am Neuen Palais 10, 14469 Potsdam, Germany

We discuss how translocation properties of the 20S proteasome influence its length distribution, one of its most important feature for the normal functioning of the immune system. For this we consider a simple one-channel proteasome model and assume that the protein transport depends significantly on the length of a protein located inside the proteasome chamber. Using the master equation approach we show analytically that the length distribution with one dominating peak, observed in the experiments, can be achieved if the transport rate function is in a certain relation with cleavage probabilities and the geometry of a proteasome. Our analytical results are confirmed by numerical simulations of the protein degradation by the proteasome performed using the modified Gillespie algorithm.

Keywords: proteasome; protein transport; peptide length distribution.

1. Introduction

Proteasomes are a class of multicatalytic cellular protease complexes that are primarily responsible for non-lysosomal protein degradation. The principle mode of occurrence of the proteasome is a proteolytically active catalytic core, also known as the 20S proteasome, or as a protein complex associated with regulatory particles, the 19S [1] and PA28 particles [2,3]. The 20S proteasome is a barrel-shaped structure composed of four stacked rings of 28 subunits [1,4]. The active cleavage sites are located within the central chamber of the 20S proteasome, into which protein substrates must enter through narrow openings of outer rings. 20S proteasomes can be found in its usual form as a constitutive proteasome, or as an immunoproteasome in which the active site subunits are replaced by IFN-γ-inducible immuno-subunits [5,6]. The capped 20S proteasomes are called 26S proteasomes, and these are thought to be responsible for the majority of the protein degradation *in vivo*, where as many experiments *in vitro* are performed with the 20S proteasomes without multiple ATP molecules present in regulating caps and without Ubiquitin.

The mechanism for protein degradation follows one of several pathways. Most proteins have to be tagged with Ubiquitin in order to be recognized and degraded by the proteasome. Proteasomes also degrade a small fraction of proteins that are

Biophysical Reviews and Letters, Vol.1, No.4 (2006) 375-386

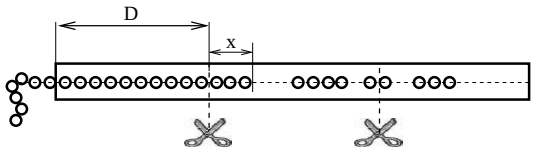

Fig. 1. Schematic diagram of the protein degradation by the proteasome. The protein strand (denoted by '0-0-0-0') enters the proteasome from the left to be cleaved by the cleavage centers (denoted by the scissors). The length of the strand after crossing the cleavage center is denoted by x.

not tagged with Ubiquitin, but this is thought to reflect a much older method of substrate recognition by the proteasomes, mediated by "built-in" sequence signals. One of the most significant effect of the proteasomal protein degradation is the formation of antigenic peptides of length $8-10$ amino-acids which are then presented by the MHC class I molecules for subsequent recognition by the T-lymphocytes [5,6,7,8,9,10]. They, therefore, form an intrinsic part of the human immune system. As a part of the Ubiquitin system, proteasomes are involved in the regulation of the cell cycle and the cell stress response. Recently, proteasome inhibition has been suggested as a promising new target for cancer treatment [11,12,13].

Due to the significance of the proteasomal protein degradation to the human immune system, the modelling of the proteasome is thought to be of primary importance in building a "virtual" immune system. However, theoretical prediction of the proteasome function and hence its effect on the human immune system is still in its infancy. There have been several approaches to modelling proteasomal protein degradation. To model the proteasome mechanism, one should adequately describe three essential processes involved in the proteasome function: i) selection of cleavage sites, ii) a peptide translocation inside the proteasome, and iii) kinetics of generated fragments. Three algorithms are available for the prediction of cleavage sites, PA-ProC [14], Netchop [15], and ProteaSMM [16]. Several theoretical models for the kinetics of proteasome degradation have been published. Some of the models describe the degradation of short peptides with qualitatively different kinetics [17,18,19] or small number of cleavage positions [20]. The theoretical model [20,21] for the degradation of long substrates is applied to specific proteins with predefined cleavage sites and is fitted to experimental data describing the fragment quantity after proteasomal degradation.

One of the important experimental result related to the theoretical modelling of the proteasome is the analysis of the length distribution of peptides produced as a result of proteasomal digestion. The experimental analysis of proteasomal cleavage products reveals a strictly non-monotonous length distribution for long substrates. The distribution has a peak around $7-12$ amino acids irrespective of the type of proteasome. Incidentally, this is also the length most frequently required for the proper functioning of the immune system. A widely accepted explanation for this

Biophysical Reviews and Letters, Vol.1, No.4 (2006) 375-386

result was a concerted cleavage, or 'molecular ruler' mechanism in which neighboring centers cleave the protein in a synchronized manner, as first proposed by [22]. However, this hypothesis was not supported by any experimental evidence and also the fact that the peak in the distributions was rounded to an extent [23]. Recently, two other mechanisms, the optimal length transportation hypothesis [24] and non-monotonous cleavage strength in kinetic models of the proteasome function [25] have been reported.

In our study we focus solely on the protein translocation and develop the idea that proteasome length distribution can be partially explained by peculiarities of the peptide translocation inside the proteasome chamber, suggested in [26,24]. We show that the differences in the length dependent velocity rates and its relation with the proteasome geometry and cleavage probabilities can be of crucial importance for the length distribution. We propose a stochastic model of proteasomal protein degradation with given cleavage probabilities and translocation rate functions that depend only on the length of the protein strand inside the proteasome. We, then, examine the model analytically, with the assumption that products of cleavage were transported out of the proteasome before undergoing further cleavage. We obtain the necessary condition for obtaining a maximum in the length distribution of peptides and find the necessary relation between the transport rate function, cleavage probabilities and the geometry of the proteasome. Finally, we find the length distributions of peptides obtained numerically to be in close agreement with our analytical results.

2. The Model

In our model we assume that the proteasome has a single channel for the entry of the substrate with two cleavage centers present at the same distance from the ends, yielding in a symmetric structure as confirmed by experimental studies of its structure. In reality a proteasome has six cleavage sites distributed spatially around its central channel. However, due to the geometry of its locations, we believe that a translocated protein meets only two of them. Whether the strand is indeed transported or cleaved at a particular position is a stochastic process with certain probabilities (see Fig. 1).

Table 1. Parameter values used in the model

Parameter	Description	Dimension	Default Value
l	Protein Length	Amino acids	200
L	Proteasome Length	Amino acids	80
D	Distance between a cleavage center and the proteasome end	Amino acids	15
N	Number of degraded proteins	-	1000
γ	Cleavage rate	-	0.001

The protein strand can be cleaved if it lies close to the cleavage center or it could be transported forward by one amino-acid. We assume that the probability of transport depends only on the length of the strand inside the proteasome. The probability of transport is, therefore, given by a translocation rate function, $v(x+D)$ where $x + D$ is the length of the strand inside the proteasome in terms of amino acids. The probability of cleavage is assumed to be a constant, denoted by γ. We also assume that the degradation of proteins by the proteasome is a highly *processive* mechanism [27], i.e., in other words, the protein is not released by the proteasome until it is completely processed. This leads to the possibility of the proteasome making several cuts in the same protein strand and in the formation of greater number of smaller length peptides. The model also does not allow cleavage products to overlap or outrun their predecessors. The standard parameters we have used for this particular model are given in Table 1.

3. Analytics - Distribution of peptide lengths

To derive analytically the proteasome length distribution, we apply the master equation approach for the distribution of the coordinate of the front end of the strand and find its stationary solution as well as the distribution of peptide length. We also assume that the products of cleavage left the chamber immediately after cleavage. This assumption can be justified by the fact that the products of cleavage have rather small size and can really left the proteasome very fast. We note that this assumption will be also motivated if the transport rate function is a monotonously decaying one, and the characteristic peptide length is small in comparison to the distance between the cleavage center and the proteasome end. In this case most of the peptides move faster than the incoming protein strand, and do not block it. Later on, using numerical simulations we compare whether this assumption can significantly change the results.

3.1. *One cleavage center*

We take the offset of the coordinate x (measured in amino acids) along the proteasome at the first cleavage center (see Fig. 1). During the time interval dt, the protein strand can move by one amino-acid with the probability $v(x + D)dt$ and can be cut with the probability γdt.

Let us have an ensemble of identical proteasomes with proteins inside, and $w(x)$ be the distribution of the proteins with the coordinate x. Then, at the x-th bond, the change in $dw(x)$ consists of the increase $v(x + D - 1)w(x - 1)dt$ due to the movement of protein ends from $x-1$ to x, the decrease $-v(x+D)w(x)dt$ due to the movement of protein ends from x to $x+1$, and the loss $-\gamma w(x)dt$ due to cleavage:

$$dw(x) = [v(x + D - 1)\, w(x - 1) - v(x + D)\, w(x)]\, dt - \gamma\, w(x)dt. \qquad (1)$$

At $x = 0$ (the protein ends at the cleavage center) we have to set the boundary condition: no strands are to be cut, and no strands move from $x = -1$ because no

Biophysical Reviews and Letters, Vol.1, No.4 (2006) 375-386

proteins end there, but there is a gain $\sum_{x=1}^{\infty}\gamma\, w(x)dt$ from cleavage, i.e.

$$dw(0) = \Big[\gamma\sum_{x=1}^{\infty} w(x) - v(D)\, w(0)\Big]dt. \tag{2}$$

Using the standard master equation technique, we consider the continuous limit, supposing that $w(x)$ and $v(x)$ vary slightly from one bond to another. Then, $\sum_{x=1}^{\infty} w(x) \approx \int_0^{\infty} w(x)dx = 1$ (the last being the normalization condition), and the discrete derivative in Eq. (1) may be replaced with the continuous derivative:

$$\dot{w}(x,t) = -\frac{\partial}{\partial x}\big(v(x+D)\, w(x,t)\big) - \gamma\, w(x,t), \tag{3}$$

with the boundary condition (2), $\dot{w}(0) = \gamma - v(D)\, w(0)$, i.e. for stationary case

$$w(0) = \frac{\gamma}{v(D)}. \tag{4}$$

The stationary solution of Eq. (3) with the boundary condition (4) gives the asymptotic distribution of protein coordinates which coincides with the length distribution of peptides $\rho(x)$ (because probability of a strand to be cut is independent of its coordinate). The problem (3),(4) admits the stationary solution

$$\rho(x) = w(x) = \frac{\gamma}{v(x+D)}\exp\Big[-\gamma\int_0^x \frac{dx'}{v(x'+D)}\Big], \tag{5}$$

thus providing us with the analytically found proteasome product length distribution.

3.2. *Two cleavage centers*

Let us now have a second cleavage center at $x_2 = L - 2D$ (see Fig. 1). If γdt is the probability of cleavage by a center during the time interval dt, then the probability of a peptide of length x to be cut by any center is $\gamma(x)dt$:

$$\gamma(x) = \begin{cases} \gamma, & 0 < x < x_2; \\ 2\gamma, & x \geq x_2. \end{cases}$$

In this case, the length distribution does not coincide with the distribution of protein coordinates. Let us start with the distribution of protein coordinates $w(x)$. Beyond the cleavage centers it obeys the equation which is similar to Eq. (3) :

$$\dot{w}(x,t) = -\frac{\partial}{\partial x}\big(v(x+D)\, w(x,t)\big) - \gamma(x)\, w(x,t). \tag{7}$$

At the first cleavage center, again, $w(0) = \gamma/v(D)$; at the second one ($x = x_2$)

$$\dot{w}(x_2) = \gamma\int_{x_2}^{\infty} w(x)dx + v(x_2+D-1)\, w(x_2-1) - v(x_2+D)\, w(x_2) - \gamma w(x_2),$$

what provides

$$w(x_2) = w(x_2-1) + \frac{u}{v(x_2+D)}, \tag{9}$$

where $u \equiv \gamma \int_{x_2}^{\infty} w(x)dx$.

So, for $x \in (0, x_2)$ the protein coordinate distribution is:

$$w(x) = w_1(x) = \frac{\gamma}{v(x+D)} \exp\Big[-\gamma \int_0^x \frac{dx'}{v(x'+D)}\Big], \tag{10}$$

and for $x \in [x_2, \infty)$, one can obtain $u = v(x_2 + D)w_1(x_2)$,

$$w_2(x) = \frac{2\gamma}{v(x+D)} \exp\Big[-\int_0^x \frac{\gamma(x')\,dx'}{v(x'+D)}\Big]. \tag{11}$$

To note, the formulae (10) and (11) may be combined:

$$w(x) = \frac{\gamma(x)}{v(x+D)} \exp\Big[-\int_0^x \frac{\gamma(x')\,dx'}{v(x'+D)}\Big]. \tag{12}$$

In its turn, the distribution of peptide lengths $\rho(x)$ is proportional to a superposition of $w(x)$ and shifted $w_2(x)$, i.e., $\rho(x) \propto w(x) + w_2(x + x_2)$, that gives us after normalization:

$$\rho(x) = \frac{w(x) + w_2(x + x_2)}{1 + e^{-\gamma \int_0^{x_2} \frac{dx'}{v(x'+D)}}}. \tag{13}$$

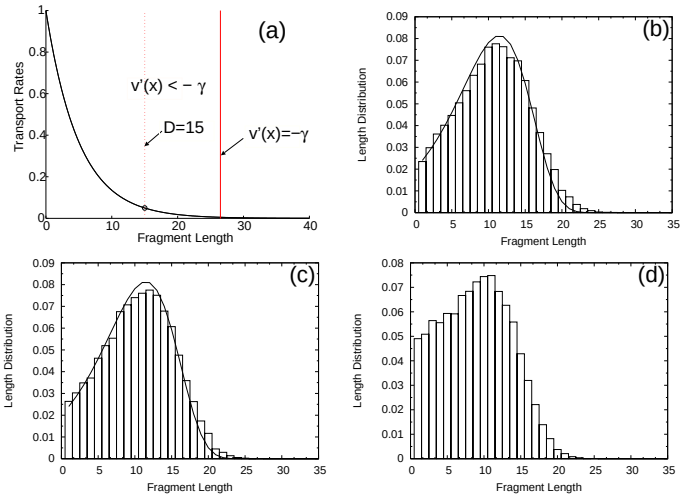

Fig. 2. (a) Monotonously decreasing transport rate function $v(x) = v_1(x)$. The vertical lines show the location of the point where the condition for the maximum in the length distribution (Eq. 15) holds and the location of the cleavage centre. The parameters are $D = 15$ and $\gamma = 0.001$. As predicted by theory (solid line) the numerically computed peptide length distribution (denoted by boxes) has a maximum for one cleavage center (b), two cleavage centers with immediate disappearance of cleavage products (c), and in the case where the cleavage products do not disappear (d).

Biophysical Reviews and Letters, Vol.1, No.4 (2006) 375-386

3.3. *Maximum in peptide length distribution*

As shown below, the presence of a second cleavage centre does not significantly change the results. Hence, to find the conditions for a maximum in the peptide length distribution, we use the analytical expressions for the case of one cleavage centre. This peptide length distribution has an extrema at the points where

$$0 = \frac{dw(x)}{dx} = \frac{\gamma}{v^2(x+D)} \exp\Big[-\gamma \int_0^x \frac{dx'}{v(x'+D)}\Big]\Big(-\frac{dv(x+D)}{dx} - \gamma\Big), \qquad (14)$$

what gives the condition for extremum,

$$\frac{dv(x+D)}{dx} = -\gamma. \qquad (15)$$

This equation should be fulfilled at least in one point for $x + D > 0$. To note γ is here the rate of cleavage. Hence, there are no limitations for its value. Eq. (15) shows that the condition for obtaining a maximum when we have a single cleavage center is independent of the actual form of the transport rate function, but is rather dependent on its slope. This would suggest that it is possible to obtain a peak in the length distribution even when the transport rate function is monotonically decreasing, and indeed that is what we find from our numerical simulations.

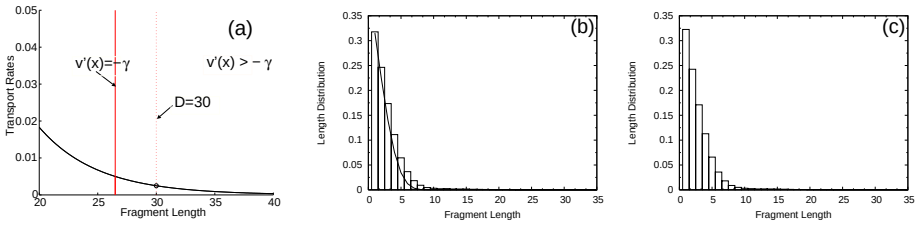

Fig. 3. (a) The case when D is large and the maximum condition holds nowhere. As predicted by the analytical theory (solid line) the length distribution does not have peaks under the assumption that the cleavage products disappear immediately (b) or without this assumption (c).

4. Comparison with numerical results

We adapt our model for numerical simulation with the help of Gillespie algorithm [28] which enables the system to jump to the next event via the calculation of the waiting time before any event will occur. Following the approach suggested by us in [24], we stochastically model the system where several events can happen with different probabilities. Suppose that on some moment of time we have a set of N probable events with rates R_i, where the $i-th$ event has the rate R_i and $i = 1..N$. Then by generating two uniformly distributed in (0, 1) random numbers RN_1 and RN_2, we estimate the time T after which the next event would occur as

$$T = -\frac{\log(RN_1)}{\sum_{i=1}^{N} R_i}. \qquad (16)$$

Biophysical Reviews and Letters, Vol.1, No.4 (2006) 375-386

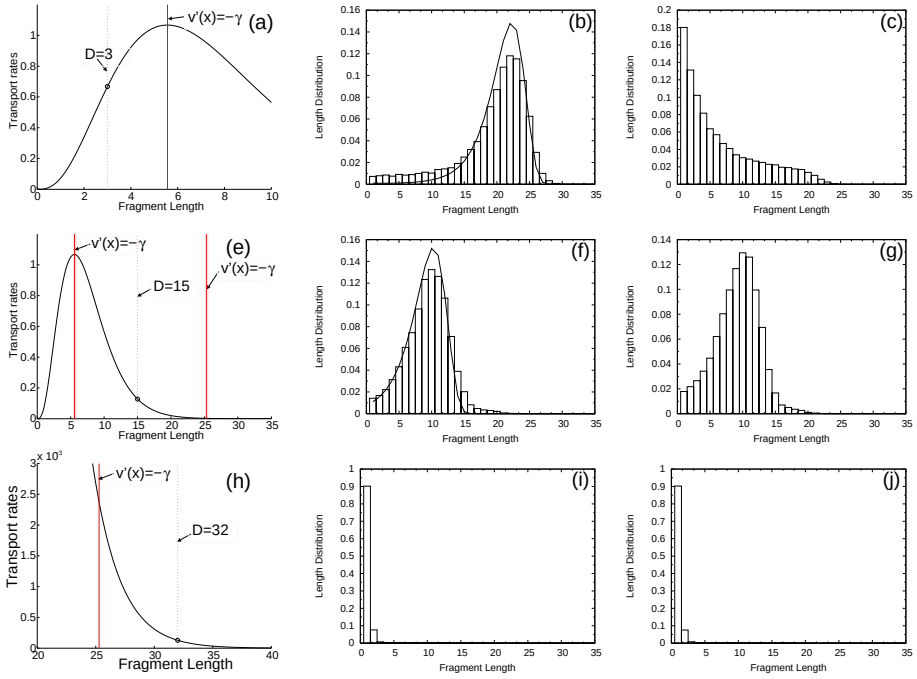

Fig. 4. The case of non-monotonous transport rate function $v_2(x)$, shown by solid line in (a,e,h). From top to bottom: different location of the cleavage centre $D = 3, 15, 32$ (shown the vertical line) with respect to two points where the condition of maximum holds (shown vertical lines); (b,f,i) the corresponding length distributions for the case of two cleavage centres. Numerics (boxes) is always in good agreement with theoretical predictions (solid line); (c,g,j) the corresponding length distribution if computed without the assumption of immediate disappearance. Only in one case (c) of rather unrealistic too small D this length distribution changes a lot from distributions (b,f,i).

The concrete event k that occurs after this time can be then found from:

$$\sum_{i=1}^{k} R_i < \sum_{i=1}^{N} R_i RN_2 \leq \sum_{i=1}^{k+1} R_i. \tag{17}$$

The peptide or its part inside the proteasome can either be shifted by one amino acid or it can be cleaved if it is located near the cleavage center. Inside the proteasome, the translocation rates of the substrate or fragments depend only on their lengths and are described by the translocation rate function $v(x + D)$ (see Fig. 1). The probability of cleavage is described by the function $R_c(p)$, where p is the position in the substrate sequence. We set the constant cleavage probability $R_c(p) = \gamma$ and discuss another situation later. When the protein is degraded, its fragments lengths are counted in the length distribution. The reliability of the results is ensured as we conduct the study over a large number of proteins N so that the trends observed in the length distribution have the basis in statistical results. To consider different situations, we study different relations between the geometry of the proteasome (the

Biophysical Reviews and Letters, Vol.1, No.4 (2006) 375-386

parameter D) and two qualitatively different transport rate functions, monotonous and non-monotonous one.

For the sake of generality we choose the following qualitatively different transport rate function:

$$v_1(x) = e^{-0.2x}, \quad v_2(x) = 0.125e^{-\alpha x}x^3, \tag{18}$$

where x is the peptide length and $\alpha = 0.54$ is a constant. It is important to note that such monotonous and non-monotonous transport functions can be obtained also if we assume that the protein translocation is driven by nonequilibrium fluctuations, as we have assumed it in [26].

4.1. *Monotonously decreasing transport rates*

First we consider a case of the monotonously decreasing transport rate function v_1. This form of function (see Fig. 2 (a)) may correspond to two different situations: when the location of the cleavage centre let the condition (Eq. 15) can be fulfilled at some point and when it cannot. The first case occurs if the parameter D is smaller than the point where the derivative of the transport function is equal to the value $-\gamma$. As predicted by the theory in this case one should observe the maximum in the length distribution. This is indeed the case, as can be shown by a comparison of the numerical results with the theoretical curve for one cleavage centre (see Fig. 2 (b)) or for two cleavage centres (see Fig. 2 (c)). It should be noted that addition of the second cleavage centre does not change the results both as predicted from the theory or computed with the Gillespie algorithm. This holds for all situations considered in this paper, hence below we plot only the results for two cleavages centers. These plots clearly show a good matching between the analytical theory developed and the results of numerical simulations. To remind, both the theory and numerical simulations have been made under the assumption that the cleavage products disappear immediately after the cut. The numerical simulations allow also to check what happens if this assumptions does not hold and the cleavage product will still move along the channel. As expected, for a monotonously decreasing transport function, the length distribution does not significantly change (see Fig. 2 (d)). This happens because the shorter cleavage products have larger probability of transport and do not stack the incoming protein.

The situation qualitatively differs if after the cleavage centre the condition of the maximum is never fulfilled. This happens if D is relatively large (see Fig. 3 (a)). In this case the length distribution would not have a maximum which is in good correspondence to the result predicted by the theory. The Fig. 3 (b) illustrates that also in this case analytical results are in good matching with numerics. The length distributions also practically do not change if the cleavage products do not disappear after the cleavage but are transported with the same rules as the incoming protein (see Fig. 3 (c)).

4.2. *Non-monotonous transport rates*

To cover several possible forms of the transport function, next we analyse the transport function $v_2(x)$ with one peak (see Fig. 4 (e)). The derivative of this function can be equal to $-\gamma$ in two points dividing all possible coordinates into three regions where the cleavage centre D can be located. Let us study these three possibilities.

First, let us consider the case when the location of the cleavage centre allows the maximum condition to be fulfilled in two points (see Fig. 4 (a)). In this case the theory predicts the non-monotonous length distribution, as confirmed also by numerics both for one or two cleavage centres (see Fig. 4 (b)). However, if we let the cleavage products do not disappear, then the length distribution is monotonously decreasing, as found by numerical simulations (see Fig. 4 (c)). This is the only case when using this assumption changes the results significantly and the theory does not predict the form of length distribution without this assumption. One should note that this case of $D = 3$ seems to be rather unrealistic, because it means that the cleavage centre is too close to the entrance what is not the case in the reality [4,1].

Next, we analyze the case, when the cleavage centre $D = 15$ is between two points where the derivative is equal to $-\gamma$, and hence the maximum condition can be fulfilled in one point (see Fig. 4 (e)). As predicted by theory and confirmed by numerics, the length distribution is to have a maximum in this case (see Fig. 4 (f)). Noteworthy, the theory in this case works sufficiently also in the case if the cleavage products do not disappear immediately (see Fig. 4 (g)). If we believe in the non-monotonous transport rate function hypothesis [24], this case seems to be the most adequate for protein degradation by the proteasome. In the last case, the cleavage centre is so deep in the proteasome $D = 32$ that the maximum condition can be fulfilled nowhere. As expected, the length distribution has no maxima in all cases computed for this relation between the transport function and the geometry of the proteasome.

5. Discussion

To summarize, we have suggested the analytical consideration of the protein translocation inside the proteasome which allows to predict the length distribution, if we know the transport rate function which depends only on the protein length. For the case of fluctuationally driven protein translocation, this function can be computed as in [26]. The main result is that the non-monotonous length distribution observed in many experiments can be the result of a certain relation between the transport function, the cleavage strength and the geometry of the proteasome structure, hence confirming and refining our previous hypothesis that length dependent translocation rates can be the reason for a non-monotonous proteasome product size distribution. The comparison between the analytical results and those of numerical simulations has revealed significant similarities when we subjected it to monotonically decreasing transport rates and non-monotonic rates. Our theory has

Biophysical Reviews and Letters, Vol.1, No.4 (2006) 375-386

been developed under the assumption that the cleavage products leave the proteasome chamber immediately and do not interact with the incoming protein strand. However, numerical simulations have shown that practically in all cases the theory makes good predictions even without this assumption except for one unrealistic case when the cleavage centre is too close to the proteasome entrance and the transport rate is non-monotonous.

One should note that many factors can influence the length distribution of the proteasome, such as translocation properties, the cleavage pattern and kinetics of the fragment production connected to different rates of influx and outflux. Here we have focused only on the influence of translocation properties. Without any doubt, one should also analyze other factors. In [24] using the numerical simulations of the same model, we have shown that the cleavage pattern may be not significant for the length distribution if the protein length is quite long (larger as 150 amino acids). Surely, for shorter proteins the influence of the cleavage pattern will dominate, but the interplay of this influence with transportation properties can be computed numerically with the same model if we set the cleavage probabilities dependent on the position along the protein strand. In the same way, one can also consider the situation when transport properties can differ a lot for different protein sequences, what can be the case for certain neurodegenerative diseases [29]. The open question is how to compile influence of translocation properties and properties of protein influx and outflux. We believe that this can be done via including transport corrections into the model of the proteasome kinetics suggested in [25].

6. Acknowledgment

AM acknowledges the University of Potsdam for financial support. AZ the VW-Stiftung, JK and AZ the EU through the Network of Excellence BioSim, Contract No. LSHB-CT-2004-005137.

References

1. O. Coux, K. Tanaka, and A. L. Goldberg, Annu. Rev. Biochem. **65**, 801 (1996).
2. M. Rechsteiner, C. Realini, and V. Ustrell, Biochem. J. **345**, 1 (2000).
3. P. M. Kloetzel, Biochem. Biophys. Acta. **1695**, 225 (2004).
4. J. M. Peters *et al.*, J. Mol. Biol. **234**, 932 (1993).
5. P. M. Kloetzel, Nat. Rev. Mol. Cell. Biol. **2**, 179 (2001).
6. P. M. Kloetzel, Nature Immunology **5**, 661 (2004).
7. K. L. Rock and A. L. Goldberg, Annu. Rev. Immunol. **17**, 739 (1999).
8. B. Lankat-Buttgereit and R. Tampe, Physiol Rev **82**, 187 (2002).
9. N. Shastri and S. Schwab, Annu. Rev. Immunol. **20**, 463 (2002).
10. A. L. Goldberg, P. Cascio, T. Saric, and K. L. Rock, Mol. Immunology **39**, 147 (2002).
11. R. Z. Orlowski, Cell Death Differ. **6**, 303 (1999).
12. J. Adams, V. Palombella, and P. Elliott, Investigational New Drugs **18**, 109 (2000).
13. Q. P. Dou, D. Smith, K. Daniel, and A. Kazi, Progress in Cell Cycle Research **5**, 441 (2003).
14. C. Kuttler *et al.*, J. Mol. Biol. **298**, 417 (2000).

15. C. Kesmir *et al.*, Protein Engineering **15**, 287 (2002).
16. S. Tenzer *et al.*, CMLS, Cell. Mol. Life Sci. **62**, 1025 (2005).
17. R. L. Stein, F. Melandri, and L. Dick, Biochemistry **35**, 3899 (1996).
18. R. Stohwasser *et al.*, Eur. J. Biochem. **267**, 6221 (2000).
19. G. Schmidtke, S. Emch, M. Groettrup, and H. G. Holzhuetter, J. Biol. Chem. **275**, 22056 (2000).
20. H. G. Holzhütter and P. M. Kloetzel, Biophysical Journal **79**, 1196 (2000).
21. B. Peters, K. Janek, U. Kuckelkorn, and H. G. Holzhütter, J. Mol. Biol. **318**, 847 (2002).
22. T. Wenzel, C. Eckerskorn, F. Lottspeich, and W. Baumeister, FEBS Letters **349**, 205 (1994).
23. A. F. Kisselev, T. N. Akopian, and A. L. Goldberg, J. Biol. Chem. **273**, 1982 (1998).
24. A. Zaikin and J. Kurths, Journal of Biological Physics (2006), accepted for publication.
25. F. Luciani *et al.*, Biophysical Journal **88**, 2422 (2005).
26. A. Zaikin and T. Pöschel, Europhysics Letters **69**, 725 (2005).
27. T. N. Akopian, A. F. Kisselev, and A. L. Goldberg, The Journal of Biological Chemistry **272**, 1791 (1997).
28. D. Gillespie, J. Comput. Phys. **22**, 403 (1976).
29. F. Luciani, M. Nielsen, C. Kesmir, and M. Di Napoli, in *The UPS in Nervous System: from Physiology To Pathology* (Nova Science Publishers, Inc, ADDRESS, 2006), Chap. Theoretical models for proteasome function: predictive methods to understand ubiquitin protein system in neurodegenerative diseases.